DALTON

Synthesis, structure and magnetism of iron-(III) and -(II) complexes of 1-thia-4,7-diazacyclononane and *N*,*N*′-dimethyl-1-thia-4,7-diazacyclononane †

Vincent A. Grillo,[a] Graeme R. Hanson,[b] Trevor W. Hambley,[c] Lawrence R. Gahan,*[,a] Keith S. Murray*[,d] and Boujemaa Moubaraki[d]

[a]*Department of Chemistry, The University of Queensland, Brisbane, QLD 4072, Australia*
[b]*Centre for Magnetic Resonance, The University of Queensland, Brisbane, QLD 4072, Australia*
[c]*School of Chemistry, The University of Sydney, Sydney, NSW 2006, Australia*
[d]*Chemistry Department, Monash University, Clayton, Victoria 3168, Australia*

The mononuclear complexes $[Fe([9]aneN_2S)Cl_3]$ and $[Fe(Me_2[9]aneN_2S)Cl_3]$ ([9]aneN$_2$S = 1-thia-4,7-diazacyclononane, $Me_2[9]aneN_2S$ = *N*,*N*′-dimethyl-1-thia-4,7-diazacyclononane) have been prepared by addition of the cyclononane to an ethanolic solution of $FeCl_3$. μ-Oxo-bis(μ-acetato)diiron(III) complexes $[Fe_2O(O_2CMe)_2([9]aneN_2S)_2][PF_6]_2$ and $[Fe_2O(O_2CMe)_2(Me_2[9]aneN_2S)_2][PF_6]_2$ have been synthesised by addition of sodium acetate to suspensions of the mononuclear complexes and isolated as the hexafluorophosphate salts. The iron(II) dimer $[Fe_2(OH)(O_2CMe)_2(Me_2[9]aneN_2S)_2]ClO_4$ was prepared under anaerobic conditions. The four iron(III) complexes were characterised by crystal structural studies. On the bases of the isomer shift and quadrupole splitting observed in the Mössbauer spectra of the dimers (4.2 K) the iron-(III) and -(II) ions were determined to be in the high-spin configuration. The magnetic susceptibility (300–4.2 K) of $[Fe_2O(O_2CMe)_2([9]aneN_2S)_2][PF_6]_2$ ($\mathcal{H} = -2JS_1 \cdot S_2$) indicated that the iron(III) sites were antiferromagnetically coupled ($J = -125$ cm^{-1}). In the case of the iron(II) dimer $J = -7.4$ cm^{-1}. The differences observed in the redox behaviour of $[Fe_2O(O_2CMe)_2([9]aneN_2S)_2][PF_6]_2$ and $[Fe_2O(O_2CMe)_2(Me_2[9]aneN_2S)_2][PF_6]_2$ are attributed to the presence of the sterically demanding ligand methyl substituents.

1,4,7-Triazacyclononane ([9]aneN$_3$) and *N*,*N*′,*N*″-trimethyl-1,4,7-triazacyclononane (Me_3[9]aneN$_3$) and their complexes with iron-(III) and -(II) have been shown to be particularly effective in the development of potential models for proteins containing the bridged iron–oxo structural motif.[1] Monomeric complexes such as $[Fe([9]aneN_3)Cl_3]$ and $[Fe(Me_3[9]aneN_3)Cl_3]$ have been shown to be useful precursors in the development of this chemistry and also to have wider synthetic application.[2–15] Derivatives of the complex $[Fe(Me_3[9]aneN_3)Cl_3]$ have been shown to be efficient DNA cleavage agents[16] and Wieghardt and co-workers[17] have shown the utility of the same complex in the generation of new complexes such as μ-nitrido-diiron systems. We have now prepared and characterised monomeric and bimetallic iron-(II) and -(III) complexes of 1-thia-4,7-diazacyclononane ([9]aneN$_2$S) and *N*,*N*′-dimethyl-1-thia-4,7-diazacyclononane (Me_2[9]aneN$_2$S), analogues of the [9]aneN$_3$ and Me_3[9]aneN$_3$ systems. We were interested to investigate the chemical influences of the thioether in the bridged diiron systems in an extension of earlier investigations related to the redox, stereochemical and spectroscopic influences on metal complexes by the replacement of nitrogen donors by thioethers.[18–24]

Experimental

Methanol and ethanol were dried over magnesium methoxide and stored under dinitrogen. Anaerobic manipulations were carried out under dry dinitrogen using standard Schlenk techniques with a double-manifold vacuum line, or in a VAC Vacuum/Atmospheres (HE-43-2) controlled-atmospheres laboratory. Electronic absorption and infrared spectra were recorded with Beckman DU7500 and Perkin-Elmer FT1600 spectrophotometers, respectively. The infrared spectra were recorded as KBr pellets. 1-Thia-4,7-diazacyclononane was prepared as previously described,[25] *N*,*N*′-dimethyl-1-thia-4,7-diazacyclononane following a previously published procedure employed for *N*-methylation of secondary amines.[26]

Syntheses

$[Fe([9]aneN_2S)Cl_3]$. A methanol solution (40 cm^3) of $FeCl_3 \cdot 6H_2O$ (2.8 g, 10.4 mmol) and 1-thia-4,7-diazacyclononane (1.46 g, 10.4 mmol) was refluxed gently for 1 h and then permitted to cool to room temperature. The orange crystalline material which precipitated was filtered off, washed with ethanol and diethyl ether and dried in air (2.9 g, 90%). The complex was recrystallised from warm acetonitrile solution (Found: C, 23.05; H, 4.6; N, 9.0. $C_6H_{14}Cl_3FeN_2S$ requires C, 23.35; H, 4.6; N, 9.1%).

$[Fe(Me_2[9]aneN_2S)Cl_3]$. The compound was prepared using a similar procedure to that employed for $[Fe([9]aneN_2S)Cl_3]$ using *N*,*N*′-dimethyl-1-thia-4,7-diazacyclononane. A bright orange microcrystalline product resulted (90%) (Found: C, 28.15; H, 5.5; N, 8.05. $C_8H_{18}Cl_3FeN_2S$ requires C, 28.55; H, 5.4; N, 8.35%).

$[Fe_2O(O_2CMe)_2([9]aneN_2S)_2][PF_6]_2$. An ethanol solution (26 cm^3) of $[Fe([9]aneN_2S)Cl_3]$ (0.5 g, 1.6 mmol) and sodium acetate (0.34 g, 4.25 mmol) was stirred for 2 h at room temperature. The resulting solution was filtered through Celite to remove precipitated sodium chloride. To the intense brown filtrate was added dropwise an ethanol solution (5 cm^3) of ammonium hexafluorophosphate (0.52 g, 3.2 mmol) producing a brown precipitate which was filtered off. The filtrate was cooled to 4 °C and upon standing for 48 h brilliant dark brown crystals deposited. The crystals were filtered off, washed with ethanol

† *Non-SI unit employed*: $\mu_B \approx 9.27 \times 10^{-24}$ J T^{-1}.

and dried in air (0.40 g, 60%) (Found: C, 23.25; H, 3.85; N, 6.0; S, 7.8. $C_{16}H_{34}F_{12}Fe_2N_4O_5P_2S_2$ requires C, 23.2; H, 4.15; N, 6.75; S, 7.75%). Absorption spectrum (MeCN): λ_{max}/nm (ε/dm^3 mol^{-1} cm^{-1}) 251 (6848), 347 (4128), 380 (sh), 430 (sh), 480 (807), 518 (sh), 564 (sh) and 740 (83). IR (KBr, cm^{-1}): ν_{asym}(CO) 1561, ν_{sym}(CO) 1420.

$[Fe_2O(O_2CMe)_2(Me_2[9]aneN_2S)_2][PF_6]_2$. This complex was prepared using a similar procedure to that for $[Fe_2O(O_2CMe)_2([9]aneN_2S)_2][PF_6]_2$ using $[Fe(Me_2[9]aneN_2S)Cl_3]$ as the starting material. Upon stirring with sodium acetate the solution turned red-brown, precipitating a pale red product upon addition of ammonium hexafluorophosphate. The compound was recrystallised by slow evaporation of an acetonitrile solution, yielding brilliant red needle-like crystals (22%) (Found: C, 27.0; H, 4.65; N, 6.2; S, 7.15. $C_{20}H_{42}F_{12}Fe_2N_4O_5P_2S_2$ requires C, 27.15; H, 4.8; N, 6.35; S, 7.25%). Absorption spectrum (MeCN): λ_{max}/nm (ε/dm^3 mol^{-1} cm^{-1}) 252 (6855), 358 (3732), 496 (873), 533 (sh) and 769 (88). IR (KBr, cm^{-1}): ν_{asym}(CO) 1542, ν_{sym}(CO) 1437.

$[Fe_2(OH)(O_2CMe)_2(Me_2[9]aneN_2S)_2]ClO_4$. All operations were carried out under anaerobic conditions. To a stirred methanol solution (25 cm^3) of *N*,*N*′-dimethyl-1-thia-4,7-diazacyclononane (1.04 g, 6 mmol) was added dropwise a methanol solution (10 cm^3) of iron(II) perchlorate hexahydrate (0.72 g, 2.0 mmol). The mixture was stirred for 1.5 h whereupon a pale green precipitate formed. Sodium acetate (0.4 g, 4.8 mmol) was then added, resulting in dissolution of the green precipitate. Upon stirring for 2 h a golden solution resulted. A methanol solution (10 cm^3) of sodium perchlorate monohydrate (0.8 g, 2.8 mmol) was added. The volume was reduced to approximately 20 cm^3 and the solution placed in a freezer at −25 °C, whereupon pale yellow crystals formed within 24 h. The product was collected and subsequently recrystallised from methanol to give pale yellow to clear crystals (Found: C, 34.65; H, 6.5; N, 7.75. $C_{20}H_{43}ClFe_2N_4O_9S_2$ requires C, 34.55; H, 6.25; N, 8.05%).

Electrochemistry

Cyclic voltammetric studies were undertaken with a BAS100B Electrochemical Analyser using a three-compartment cell. A glassy carbon working electrode, platinum-wire auxiliary and a Ag–Ag$^+$ (0.01 mol dm^{-3} $AgNO_3$ in acetonitrile) reference electrode were employed. All solutions were degassed by purging with nitrogen for at least 15 min prior to the experiment. Acetonitrile were dried and distilled prior to use. The ferrocenium–ferrocene couple was employed as an internal reference.

Magnetic studies

Magnetic susceptibility studies were made using a Quantum Design MPMS SQUID magnetometer with an applied field of 1 T. The powdered sample was contained in a calibrated gelatine capsule held in the centre of a soda straw fixed to the end of the sample rod. The magnetisation values of the instrument were calibrated against a standard palladium sample, supplied by Quantum Design, and also chemical calibrants such as $CuSO_4 \cdot 5H_2O$ and $[Ni(en)_3][S_2O_3]$ (en = ethane-1,2-diamine).

Mössbauer spectroscopy

Mössbauer spectra were measured in the Physics Department at Monash University with a standard electromechanical transducer operating in a symmetrical constant-acceleration mode. A conventional helium-bath cryostat was employed for temperature control with the sample maintained in exchange gas. Data were collected with an LSI-based 1000-channel multichannel analyser. Velocity calibration was made with respect to iron foil. Spectra were fitted with a Lorentzian lineshape.

Crystallography

Data collection, structure solution and refinement. Crystal data and refinement details for the complexes $[Fe([9]aneN_2S)Cl_3]$, $[Fe(Me_2[9]aneN_2S)Cl_3]$ and $[Fe_2O(O_2CMe)_2([9]aneN_2S)_2][PF_6]_2$, $[Fe_2O(O_2CMe)_2(Me_2[9]aneN_2S)_2][PF_6]_2$ are reported in Table 1. For diffractometry crystals were mounted on glass fibres with cyanoacrylate resin. Lattice parameters at 294 K were determined by least-squares fits to the setting parameters of 25 independent reflections, measured and refined on an Enraf-Nonius CAD4-F four-circle diffractometer with a graphite monochromator (Mo-Kα, λ 0.710 69 Å). Intensity data were collected in the range $1 < \theta < 25°$. Data were reduced and Lorentz-polarisation and numerical absorption corrections applied using the SDP package.[27] The structures were solved using direct methods in SHELXS 86[28] and refined (on *F*) by full-matrix least-squares analysis with SHELX 76.[29] Neutral complex scattering factors were used.[30] Hydrogen atoms were included at calculated sites with fixed isotropic thermal parameters. All other atoms were refined anisotropically. Plots were drawn using ORTEP.[31] Selected bond lengths and angles are given in Tables 2–5.

Atomic coordinates, thermal parameters, and bond lengths and angles have been deposited at the Cambridge Crystallographic Data Centre (CCDC). See Instructions for Authors, *J. Chem. Soc., Dalton Trans.*, 1997, Issue 1. Any request to the CCDC for this material should quote the full literature citation and the reference number 186/319.

Results and Discussion

Syntheses

The mononuclear complexes $[Fe([9]aneN_2S)Cl_3]$ and $[Fe(Me_2[9]aneN_2S)Cl_3]$, employed as starting materials for the syntheses of the dimers, were prepared by either addition of the desired cyclononane to an ethanolic solution of hydrated iron(III) chloride, or gentle reflux of a methanolic solution of the chloride and the macrocycle.[15] Recrystallisation of $[Fe([9]aneN_2S)Cl_3]$ and $[Fe(Me_2[9]aneN_2S)Cl_3]$ by slow evaporation of either acetonitrile or methanol solutions afforded crystals of X-ray crystallographic quality. Addition of sodium acetate to suspensions of $[Fe([9]aneN_2S)Cl_3]$ or $[Fe(Me_2[9]aneN_2S)Cl_3]$ in ethanol, removal of any precipitates, and addition of ammonium hexafluorophosphate resulted in crystallisation of $[Fe_2O(O_2CMe)_2([9]aneN_2S)_2][PF_6]_2$ and $[Fe_2O(O_2CMe)_2(Me_2[9]aneN_2S)_2][PF_6]_2$, respectively. The synthetic methodology is similar to that reported for the μ-oxo-bis(μ-acetato)diiron(III) compounds $[Fe_2O(O_2CMe)_2([9]aneN_3)_2]I_2$ and $[Fe_2O(O_2CMe)_2\{HB(pz)_3\}_2]$ (pz = pyrazolyl).[12,32] The lability of the chlorides, and the stability of the μ-oxo-bis(μ-acetato) core, ensured the production of both $[Fe_2O(O_2CMe)_2([9]aneN_2S)_2][PF_6]_2$ and $[Fe_2O(O_2CMe)_2(Me_2[9]aneN_2S)_2][PF_6]_2$ in moderate to good yields. The synthesis of the iron(II) complex $[Fe_2(OH)(O_2CMe)_2(Me_2[9]aneN_2S)_2]ClO_4$ was achieved under anaerobic conditions although crystals suitable for X-ray analysis were not obtained.

Crystal structures

Crystal data for the iron(III) complexes are given in Table 1. The structures and atom numbering schemes for $[Fe([9]aneN_2S)Cl_3]$ and $[Fe(Me_2[9]aneN_2S)Cl_3]$ are shown in Figs. 1 and 2, respectively, while selected bond lengths and angles are in Tables 2 and 3. The structures are composed of the cyclononane ligand, an iron(III) atom and three chloride atoms. In both, the cyclononane ligands occupy three co-ordination sites about iron(III), with the three chloride ions completing the distorted octahedron. The addition of the *N*-methyl substituents makes very little difference to the N–Fe–N and N–Fe–S bond angles which are similar in both structures, as are the Cl–Fe–Cl bond angles. A slight elongation (0.08 Å) is observed in the Fe–N bond

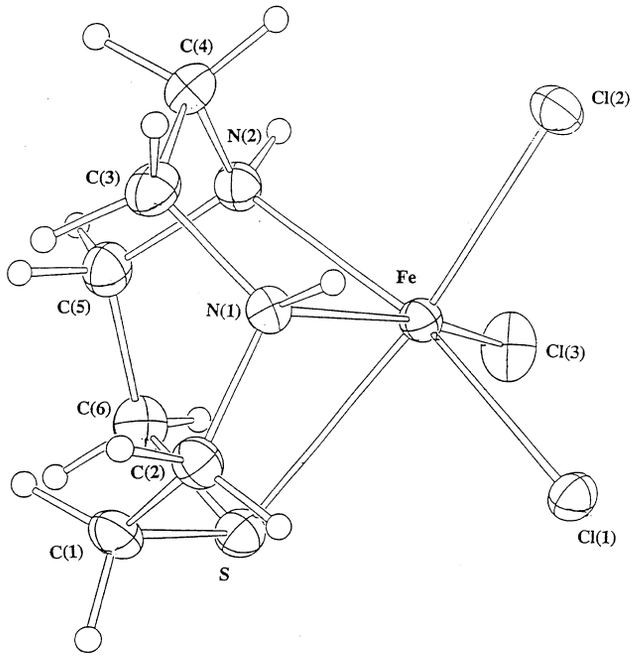

Fig. 1 Structure of $[Fe([9]aneN_2S)Cl_3]$ with relevant atoms labelled. 30% Probability ellipsoids are shown

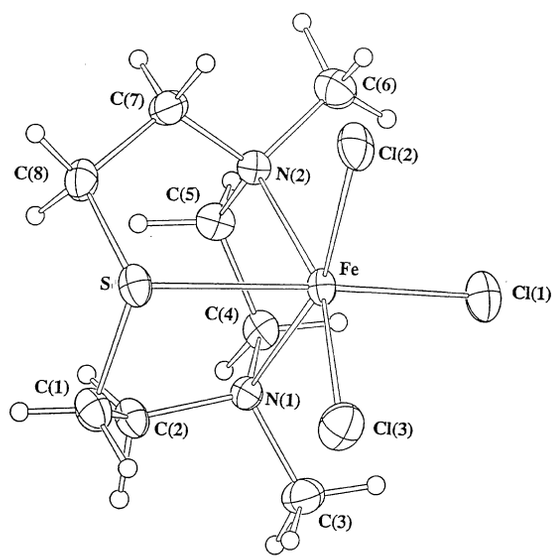

Fig. 2 Structure of $[Fe(Me_2[9]aneN_2S)Cl_3]$. Details as in Fig. 1

distance on going from $[Fe([9]aneN_2S)Cl_3]$ to the *N*-methylated analogue, $[Fe(Me_2[9]aneN_2S)Cl_3]$, but both are shorter than those observed for $[Fe(Me_3[9]aneN_3)Cl_3]$ (2.232–2.264 Å).[16] The Fe^{III}–S bond lengths exhibited by these complexes appear typical of the few examples reported previously.[33–35] The Fe–Cl bond distances are within the range of previously reported Fe–Cl bond distances.[36,37] The related complex $[Fe\{HB(pz)_3\}Cl_3]^-$ exhibits Fe–Cl bond distances of 2.319(1), 2.316(1) and 2.305(1) Å, the shorter being associated with the longer *trans* Fe–N bond.[36] The Fe–Cl bond lengths in $[Fe([9]aneN_2S)Cl_3]$ and $[Fe(Me_2[9]aneN_2S)Cl_3]$ are essentially equivalent (average 2.303 and 2.291 Å, respectively), although a small elongation of that adjacent to the thioether is observed, possibly attributed to steric effects between the thioether and the chloride. The Fe–Cl bond lengths for $[Fe(Me_3[9]aneN_3)Cl_3]$ range from 2.300 to 2.309 Å.[16]

The structures and atom numbering schemes for $[Fe_2O(O_2CMe)_2([9]aneN_2S)_2][PF_6]_2$ and $[Fe_2O(O_2CMe)_2(Me_2[9]aneN_2S)_2][PF_6]_2$ are shown in Figs. 3 and 4, respectively, while selected bond lengths and angles are given in Tables 4 and 5. It is generally observed that the Fe···Fe distances for the μ-oxo-μ-acetato binuclear complexes with the cyclononane ligands are shorter than for other complexes containing this bridging core.[14] The Fe···Fe distances for $[Fe_2O(O_2CMe)_2([9]aneN_2S)_2][PF_6]_2$ and $[Fe_2O(O_2CMe)_2(Me_2[9]aneN_2S)_2][PF_6]_2$ [3.057(2) and 3.076(3) Å, respectively] reflect a lengthening upon addition of the *N*-methyl groups. The effect is not as pronounced as for the $[9]aneN_3$ analogues where the increase in Fe···Fe distance between $[Fe_2O(O_2CMe)_2([9]aneN_3)_2][PF_6]_2$ and $[Fe_2O(O_2CMe)_2(Me_3[9]aneN_3)_2][PF_6]_2$ was 3.063(5)[2] and 3.12(1) Å.[14] The $Me_2[9]aneN_2S$ ligand appears to offer less steric repulsion than the $Me_3[9]aneN_3$ analogue.

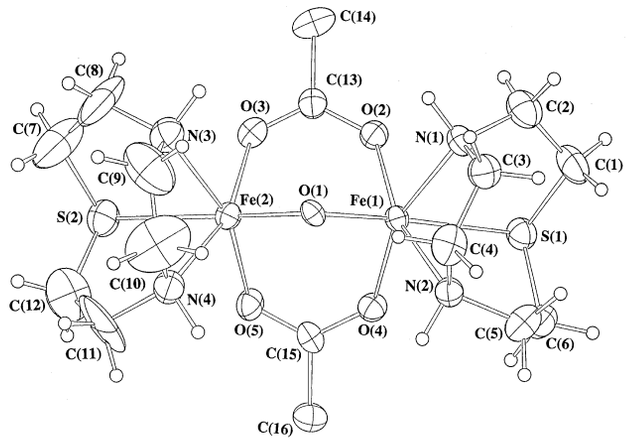

Fig. 3 Structure of $[Fe_2O(O_2CMe)_2([9]aneN_2S)_2][PF_6]_2$. Details as in Fig. 1

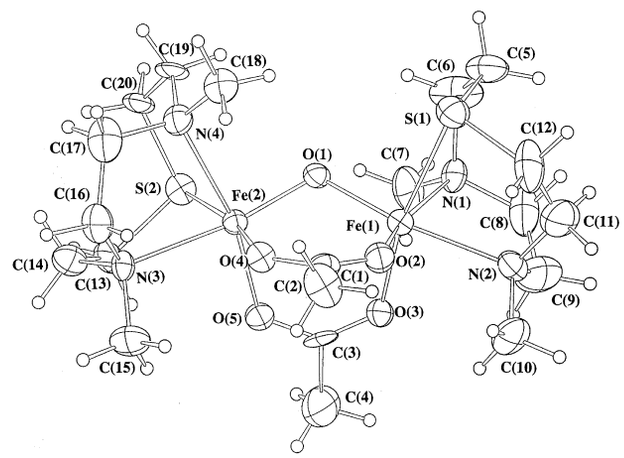

Fig. 4 Structure of $[Fe_2O(O_2CMe)_2(Me_2[9]aneN_2S)_2][PF_6]_2 \cdot MeCN$. Details as in Fig. 1

It was anticipated that a distribution of products might be observed with the mixed sulfur–nitrogen ligands, with the thioether donors being *cis* and/or *trans* with respect to the bridging oxo moiety, and in a *gauche*, *anti* or *syn* arrangement with respect to the Fe–O–Fe projection. However, for the $[Fe_2O(O_2CMe)_2([9]aneN_2S)_2]^{2+}$ complex the crystal structure indicated that the product isolated displayed the thioethers *trans* with respect to the bridging oxo unit, with S–Fe–O bond angles of 175.5(2) and 178.2(2)° and in a *syn* configuration with respect to the Fe–O–Fe plane. However, for the analogous $[Fe_2O(O_2CMe)_2(Me_2[9]aneN_2S)_2]^{2+}$ complex the structural analysis indicated that the thioethers were located *cis* to the bridging oxo group, and in a *gauche* configuration with respect to the Fe–O–Fe plane. The solid-state structure, of course, does not necessarily reflect that which exists in solution.

Table 1 Crystal data for the complexes

	[Fe([9]aneN$_2$S)Cl$_3$]	[Fe(Me$_2$[9]aneN$_2$S)Cl$_3$]	[Fe$_2$O(O$_2$CMe)$_2$([9]aneN$_2$S)$_2$][PF$_6$]$_2$	[Fe$_2$O(O$_2$CMe)$_2$(Me$_2$[9]aneN$_2$S)$_2$][PF$_6$]$_2$·MeCN
Empirical formula	$C_6H_{14}Cl_3FeN_2S$	$C_8H_{18}Cl_3FeN_2S$	$C_{16}H_{34}F_{12}Fe_2N_4O_5P_2S_2$	$C_{22}H_{45}F_{12}Fe_2N_5O_5P_2S_2$
M	308.46	336.52	828.23	926.06
Crystal system	Monoclinic	Monoclinic	Monoclinic	Orthorhombic
Space group	$P2_1/n$	$P2_1/n$	$P2_1/c$	$Pcab$
a/ Å	7.994(1)	7.326(1)	11.039(2)	14.512(4)
b/ Å	13.443(2)	12.611(3)	14.218(4)	17.569(4)
c/ Å	11.122(1)	14.628(3)	40.648(10)	29.612(6)
β/°	92.50(1)	91.06(1)	90.41(2)	
U/Å^3	1194.1(3)	1351.3(4)	6379(3)	7550(3)
Z	4	4	8	8
D_c/g cm^{-3}	1.716	1.654	1.725	1.630
μ/cm^{-1}	19.99	17.70	15.02	10.49
F(000)	628	692	3360	3696
Crystal colour	Orange	Orange	Brown	Red-brown
Habit	Prismatic	Prism	Needles	Needles
Dimensions/mm	0.22 × 0.15 × 0.13	0.13 × 0.14 × 0.23	0.11 × 0.30 × 0.13	0.25 × 0.07 × 0.05
Scan mode	ω–2θ	ω–θ	ω–θ	ω–θ
θ Range/°	1.0–27.5	1–27.5	1–22.5	1.0–22
Reflections measured	3003	3360	8956	5023
hkl Ranges	−10 to 10, 0–17, 0–14	−9 to 9, 0–16, 0–19	−11 to 11, 0–15, 0–43	0–15, 0–18, 0–31
Merging R	0.021	0.016	0.032	
Reflections used [$I > 2.5\sigma(I)$]	2400	2269	4116	1377
Number of variables	175	209	797	483
$R(F_o)$	0.021	0.031	0.064	0.051
R'	0.025	0.034	0.069	0.051
g, k in $w = g/[\sigma^2(F_o) + kF_o^2]$	1.58, 8.0 × 10^{-5}	1.53, 1.55 × 10^{-4}	3.04, 5.4 × 10^{-4}	1.49, 4.0 × 10^{-4}
Shift/e.s.d.	0.007	0.006	0.2	0.06
Residual extrema/e Å^{-3}	0.37, −0.23	0.42, −0.32	0.52, −0.43	0.41, 0.28

Table 2 Selected bond lengths (Å) and angles (°) for [Fe([9]aneN$_2$S)Cl$_3$]

Cl(1)–Fe	2.331(0)	Cl(2)–Fe	2.279(0)
Cl(3)–Fe	2.298(0)	S–Fe	2.549(0)
N(1)–Fe	2.195(1)	N(2)–Fe	2.199(2)
Cl(2)–Fe–Cl(1)	96.3(0)	Cl(3)–Fe–Cl(1)	99.1(0)
Cl(3)–Fe–Cl(2)	100.3(0)	S–Fe–Cl(1)	88.7(0)
S–Fe–Cl(2)	171.1(0)	S–Fe–Cl(3)	86.1(0)
N(1)–Fe–Cl(1)	91.2(0)	N(1)–Fe–Cl(2)	92.9(0)
N(1)–Fe–Cl(3)	162.2(0)	N(1)–Fe–S	79.6(0)
N(2)–Fe–Cl(1)	165.2(0)	N(2)–Fe–Cl(2)	92.6(0)
N(2)–Fe–Cl(3)	90.9(0)	N(2)–Fe–S	81.1(0)
N(2)–Fe–N(1)	76.5(1)		

Table 3 Selected bond lengths (Å) and angles (°) for [Fe(Me$_2$[9]aneN$_2$S)Cl$_3$]

Cl(1)–Fe	2.274(1)	Cl(2)–Fe	2.312(1)
Cl(3)–Fe	2.288(1)	S–Fe	2.516(1)
N(1)–Fe	2.273(2)	N(2)–Fe	2.279(2)
Cl(2)–Fe–Cl(1)	99.0(1)	Cl(3)–Fe–Cl(1)	98.2(1)
Cl(3)–Fe–Cl(2)	97.6(1)	S–Fe–Cl(1)	173.0(1)
S–Fe–Cl(2)	87.2(1)	S–Fe–Cl(3)	84.2(1)
N(1)–Fe–Cl(1)	92.4(1)	N(1)–Fe–Cl(2)	162.5(1)
N(1)–Fe–Cl(3)	93.9(1)	N(1)–Fe–S	80.8(1)
N(2)–Fe–Cl(1)	96.0(1)	N(2)–Fe–Cl(2)	88.7(1)
N(2)–Fe–Cl(3)	163.3(1)	N(2)–Fe–S	80.7(1)
N(2)–Fe–N(1)	76.8(1)		

For [Fe$_2$O(O$_2$CMe)$_2$(Me$_2$[9]aneN$_2$S)$_2$][PF$_6$]$_2$ the average Fe–S bond distance is 2.516(6) Å increasing to an average of 2.573(4) Å for the Fe–S bond *trans* to the μ-oxo in [Fe$_2$O(O$_2$CMe)$_2$([9]aneN$_2$S)$_2$][PF$_6$]$_2$, a difference ascribed to the *trans* influence of the oxo group.[32] A smaller change is observed for [Fe$_2$O(O$_2$CMe)$_2$(Me$_2$[9]aneN$_2$S)$_2$][PF$_6$]$_2$, which contains Fe–N bonds both *cis* [Fe–N 2.230(14) Å] and *trans* [2.256(16) Å] to the μ-oxo unit. The Fe–S and Fe–N bond lengths in the dimeric complexes are similar to those observed in the mononuclear complexes, [Fe([9]aneN$_2$S)Cl$_3$] and [Fe(Me$_2$[9]aneN$_2$S)Cl$_3$], although lengthening of the *trans* μ-oxo Fe–N in [Fe$_2$O(O$_2$CMe)$_2$(Me$_2$[9]aneN$_2$S)$_2$][PF$_6$]$_2$ and the Fe–S *trans* μ-oxo in the [Fe$_2$O(O$_2$CMe)$_2$([9]aneN$_2$S)$_2$][PF$_6$]$_2$ is observed. These differences are again ascribed to the *trans* influence of the μ-oxo compared to the μ-carboxylato group, and similar effects have been reported previously for the related [Fe$_2$O(O$_2$CMe)$_2$\{HB(pz)$_3$\}$_2$] complex.[32]

The Fe–O–Fe angles for both compounds are similar, 118.5(4)° for [Fe$_2$O(O$_2$CMe)$_2$([9]aneN$_2$S)$_2$]$^{2+}$ and 118.4(5)° for [Fe$_2$O(O$_2$CMe)$_2$(Me$_2$[9]aneN$_2$S)$_2$]$^{2+}$, and fall within the range reported for related complexes.[2,3]

Table 4 Selected bond lengths (Å) and angles (°) for [Fe$_2$O(O$_2$CMe)$_2$([9]aneN$_2$S)$_2$][PF$_6$]$_2$

Fe(2) · · · Fe(1)	3.057(2)	S(1)–Fe(1)	2.590(4)
N(1)–Fe(1)	2.150(9)	N(2)–Fe(1)	2.155(9)
O(1)–Fe(1)	1.774(7)	O(2)–Fe(1)	2.002(8)
O(4)–Fe(1)	2.004(7)	S(2)–Fe(2)	2.563(4)
N(3)–Fe(2)	2.164(11)	N(4)–Fe(2)	2.141(11)
O(1)–Fe(2)	1.783(7)	O(3)–Fe(2)	2.038(9)
O(5)–Fe(2)	2.005(8)	C(16)–C(15)	1.507(17)
C(13)–O(2)	1.257(14)	C(14)–C(13)	1.552(19)
C(15)–O(5)	1.267(14)	C(13)–O(3)	1.235(16)
C(15)–O(4)	1.265(14)		
N(1)–Fe(1)–S(1)	80.8(3)	N(2)–Fe(1)–Fe(2)	115.9(3)
O(1)–Fe(1)–N(1)	98.7(3)	O(1)–Fe(1)–S(1)	175.5(2)
O(2)–Fe(1)–N(1)	87.0(3)	O(1)–Fe(1)–N(2)	93.4(3)
O(2)–Fe(1)–O(1)	96.6(3)	O(2)–Fe(1)–S(1)	87.8(2)
O(4)–Fe(1)–S(1)	81.4(2)	O(2)–Fe(1)–N(2)	163.9(3)
O(4)–Fe(1)–N(2)	88.8(3)	O(4)–Fe(1)–O(1)	98.2(3)
O(4)–Fe(1)–O(2)	102.1(3)	O(4)–Fe(1)–N(1)	159.7(3)
N(4)–Fe(2)–N(3)	78.9(4)	N(3)–Fe(2)–S(2)	80.5(3)
O(1)–Fe(2)–S(2)	178.2(2)	N(4)–Fe(2)–S(2)	81.7(3)
O(1)–Fe(2)–N(4)	97.5(4)	O(1)–Fe(2)–N(3)	97.8(4)
O(3)–Fe(2)–S(2)	84.5(2)	O(3)–Fe(2)–N(3)	87.9(4)
O(3)–Fe(2)–N(4)	162.2(4)	O(3)–Fe(2)–O(1)	96.0(3)
O(5)–Fe(2)–S(2)	83.2(2)	O(5)–Fe(2)–O(3)	100.2(3)

Table 5 Selected bond lengths (Å) and angles (°) for $[Fe_2O(O_2CMe)_2(Me_2[9]aneN_2S)_2][PF_6]_2$

Fe(2) · · · Fe(1)	3.076(3)	N(1)–Fe(1)	2.230(14)
O(1)–Fe(1)	1.799(10)	S(2)–Fe(2)	2.520(5)
O(3)–Fe(1)	1.946(12)	O(4)–Fe(2)	2.034(11)
N(2)–Fe(1)	2.256(16)	N(3)–Fe(2)	2.265(14)
O(1)–Fe(2)	1.782(10)	C(1)–O(2)	1.194(25)
O(5)–Fe(2)	2.006(11)	C(1)–O(4)	1.294(23)
N(4)–Fe(2)	2.240(15)	C(3)–O(3)	1.239(25)
C(3)–O(5)	1.259(23)	C(2)–C(1)	1.470(29)
C(4)–C(3)	1.548(29)	S(1)–Fe(1)	2.511(6)
O(2)–Fe(1)	1.984(13)		
O(2)–Fe(1)–S(1)	85.6(4)	O(2)–Fe(1)–O(1)	98.3(5)
O(1)–Fe(1)–S(1)	91.7(4)	O(3)–Fe(1)–S(1)	168.6(4)
O(3)–Fe(1)–O(1)	99.3(5)	O(3)–Fe(1)–O(2)	95.6(5)
N(1)–Fe(1)–O(1)	93.9(5)	N(1)–Fe(1)–S(1)	83.0(4)
N(1)–Fe(1)–O(3)	93.3(5)	N(1)–Fe(1)–O(2)	163.5(5)
N(2)–Fe(1)–S(1)	82.6(4)	N(2)–Fe(1)–O(1)	171.8(5)
N(2)–Fe(1)–O(2)	87.2(6)	N(2)–Fe(1)–O(3)	86.1(6)
N(2)–Fe(1)–N(1)	79.6(6)	O(1)–Fe(2)–S(2)	93.2(4)
O(4)–Fe(2)–O(1)	97.5(5)	O(4)–Fe(2)–S(2)	169.3(4)
O(5)–Fe(2)–O(1)	98.5(5)	Fe(2)–O(1)–Fe(1)	118.4(5)
O(5)–Fe(2)–O(4)	94.2(5)		

The Fe–O bond distances for the complex $[Fe_2O(O_2CMe)_2([9]aneN_2S)_2][PF_6]_2$, (average 1.78 Å) and $[Fe_2O(O_2CMe)_2(Me_2[9]aneN_2S)_2][PF_6]_2$ (average 1.89 Å) are similar to those reported for $[Fe_2O(O_2CMe)_2([9]aneN_3)_2]I_2\cdot 0.5MeCN$ and the methylated analogue $[Fe_2O(O_2CMe)_2(Me_3[9]aneN_3)_2][ClO_4]_2\cdot H_2O$ [1.781(4) and 1.800(3) Å, respectively].[13,14]

Complexes with both symmetrically and unsymmetrically substituted μ-oxo-μ-carboxylato cores have been prepared and in each case the dimensions of the core remain essentially the same, indicating that the nature of the terminal ligands does not affect the dimensions of this core.[38,39]

Mössbauer spectroscopy

The Mössbauer spectra of $[Fe_2O(O_2CMe)_2([9]aneN_2S)_2][PF_6]_2$ and $[Fe_2O(O_2CMe)_2(Me_2[9]aneN_2S)_2][PF_6]_2$ at 4.2 K and zero field consist of a symmetric quadrupole doublet with an isomer shift of 0.48 and 0.49 mm s^{-1}, respectively. The observed isomer shifts are in the range 0.35–0.60 mm s^{-1}, characteristic of five- or six-co-ordinate high-spin iron(III) μ-oxo compounds.[3,14,40] The isomer shift indicates a similar electron density around the iron atoms, and appears insensitive to the terminal ligands. The quadrupole doublet is not distinctive with values of 1.23 and 1.52 mm s^{-1} for $[Fe_2O(O_2CMe)_2([9]aneN_2S)_2][PF_6]_2$ and $[Fe_2O(O_2CMe)_2(Me_2[9]aneN_2S)_2][PF_6]_2$, respectively. The quadrupole splitting for the two compounds agree well with those of other Fe–O–Fe compounds in the high-spin state.[14,40]

The isomer shift and quadrupole splitting for $[Fe_2(OH)(O_2CMe)_2(Me_2[9]aneN_2S)_2]ClO_4$ were 1.19 and 2.67 mm s^{-1}, similar to those reported for $[Fe_2(OH)(O_2CMe)_2(Me_3[9]aneN_3)_2]ClO_4$ (1.16 and 2.83 mm s^{-1}, respectively).[14] The values are consistent with iron(II) in the high-spin configuration and are in agreement with values reported for other binuclear high-spin iron(II) complexes.[3,40,41]

Magnetic susceptibility

The magnetic susceptibility of the binuclear iron compound $[Fe_2O(O_2CMe)_2([9]aneN_2S)_2][PF_6]_2$ was analysed using the spin-exchange Hamiltonian, $\hat{H} = -2JS_1\cdot S_2$ ($S_1 = S_2 = \frac{5}{2}$). Additional terms for the temperature-independent paramagnetism and the mole percentage of paramagnetic impurity, *p*, were included in the susceptibility expression.[42] Plots of molar susceptibility and effective moment *versus* temperature are given in Fig. 5. The best least-squares fit obtained gave $J = -125$ cm^{-1}, $p = 0.37\%$, $g = 2.078$ and $\theta = -30$ K, where θ is incorporated in the $T - \theta$ term.

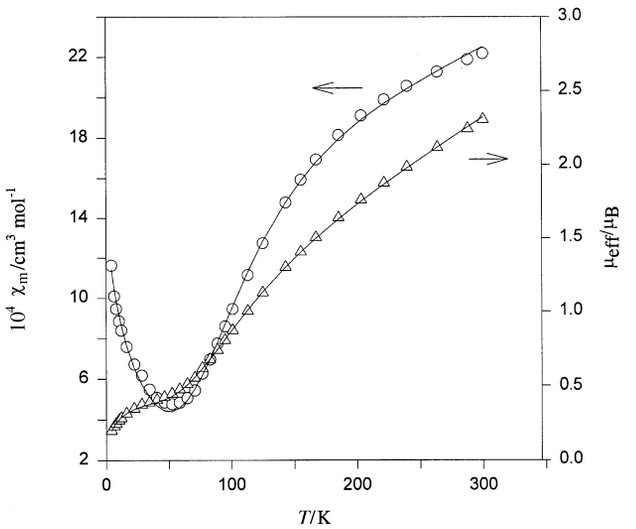

Fig. 5 Plot of χ_m and μ_{eff} *vs.* *T* for $[Fe_2O(O_2CMe)_2([9]aneN_2S)_2][PF_6]_2$. The solid line represents the best least-squares fit to the experimental data using the parameters given in the text

Measurements on two samples of $[Fe_2O(O_2CMe)_2(Me_2[9]aneN_2S)_2][PF_6]_2$ unfortunately gave magnetisation values very similar to those of the sample holder and thus the resultant molar susceptibilities were not as well defined as in the $[9]aneN_2S$ example. Nevertheless, a *J* value of *ca.* -130 cm^{-1} could be deduced from the high-temperature data but with a *g* value much lower than expected, *viz.* ≈1.5. The possibility of cocrystallisation of some diamagnetic diluent seems unlikely in view of the very good microanalytical data obtained.

Invariably, the magnetic exchange coupling in the binuclear μ-oxo-diiron(III) complexes is antiferromagnetic giving rise to an $S = 0$ ground state. For binuclear μ-oxo-bis(μ-acetato)diiron(III) complexes the magnitude of the coupling falls in the range -84 cm^{-1} for $[Fe_2O(O_2CMe)_2([9]aneN_3)_2]I_2\cdot 0.5NaI\cdot 3H_2O$ to -132 cm^{-1} for $[Fe_2(bipy)_2O(O_2CMe)_2Cl_2]$ (bipy = 2,2′-bipyridyl),[15,39,43] with values of -120 to -130 cm^{-1} being most common[39] for these model compounds and for the diiron(III) forms of iron–oxo proteins.[1] The apparent invariance of the magnitude and the size of the electron exchange between the two high-spin iron(III) ions through the μ-oxo-bis(μ-acetato) core, even upon introduction of a thioether donor to the terminal ligand, illustrates both the stability of the core and its dominance in the mediation of the electron exchange. The large negative θ value was required to obtain the fit and reproduce the small decrease in moment below 20 K. A similar constraint was observed in the magnetic studies with $[Fe_2O(O_2CMe)_2(Me_3[9]aneN_3)_2][PF_6]_2$ ($J = -119$ cm^{-1}, $\theta = -37$ K).[14]

The mechanism of exchange, and the correlation of structural features to the magnitude and the sign of the exchange in binuclear iron(III) complexes, has in recent years received considerable attention.[44–52] In general, evidence points to a correlation, especially in multiply bridged systems, between the Fe–O bond distance (or distance with the shortest superexchange pathway), rather than the Fe–O–Fe bond angle, and the exchange coupling constant. A recent study by Wieghardt and co-workers[2] proposed a theory for the observed invariance of the Fe–O–Fe angle with the exchange coupling parameter. It was suggested that the major pathways are the orbital interactions of β_{yz-yz} and $\beta_{xz-z^2} = \beta_{z^2-xz}$ producing antiferromagnetic interactions $J_{z^2-xz}^{AF}$, $J_{xz-z^2}^{AF}$ and J_{yz-yz}^{AF}. Using Hückel calculations for the N_5Fe^{III}–$Fe^{III}N_5$ model it was shown that these interactions were the major terms and the $\beta_{z^2-z^2}$ was approximately four times weaker.[2] The Fe^{III}–O–Fe^{III} system remains strongly antiferromagnetic because the S_{yz-yz} (S_{ij} being the orbital overlap integral) is not angular dependent. As the M–O–M angle increases the value of $J_{xz-z^2}^{AF}$ decreases, but the value of J_{xz-xz}^{AF} increases and maintains the strong antiferro-

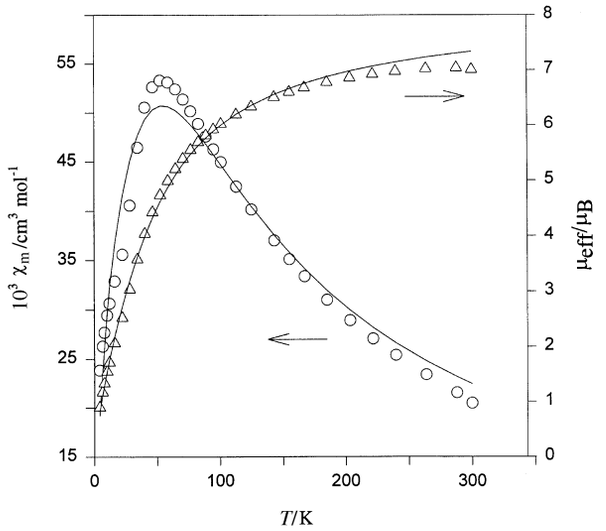

Fig. 6 Plots of χ_m and μ_{eff} *vs.* T for $[Fe_2(OH)(O_2CMe)_2(Me_2[9]aneN_2S)_2]ClO_4$. Details as in Fig. 5

magnetic coupling. Similarly, the $S_{z^2-z^2}$ overlap is expected to increase, further compensating for the decrease in S_{xz-z^2}.[2]

Gorun and Lippard[47] also investigated the antiferromagnetic coupling of di- and tri-bridged high-spin iron(III) complexes. It was concluded that for binuclear iron(III) complexes with μ-oxo (μ-hydroxo, alkoxo) and at least one other bridging ligand (carboxylate, sulfate, *etc.*), a correlation existed between the antiferromagnetic exchange coupling and P, defined as half the shortest superexchange pathway between the two iron(III) ions. The relationship proposed was $-J = A\exp(BP)$, where $A = 8.763 \times 10^{11}$ and $B = -12.663$ and are numerical constants.[47] No correlation of the coupling constant with the Fe–O–Fe angle was found. Application of this correlation to $[Fe_2O(O_2CMe)_2([9]aneN_2S)_2][PF_6]_2$, using the determined Fe–O bond distance of 1.779 Å, produced a value of $J = -144$ cm^{-1}, 10% greater than the experimentally determined value (-125 cm^{-1}).

The exchange coupling for $[Fe_2(OH)(O_2CMe)_2(Me_2[9]aneN_2S)_2]ClO_4$ was analysed using $S_1 = S_2 = 2$ ($\mathcal{H} = -2JS_1 \cdot S_2$) model.[42] The best least-squares fit obtained gave $J = -7.4$ cm^{-1}, $g = 2.23$ and $\theta = -1.5$ K. Plots for molar susceptibility and effective moment *versus* temperature are given in Fig. 6. The maximum in χ_m at *ca.* 50 K is indicative of weak antiferromagnetic coupling. Below this maximum the observed data reproducibly show a change in slope at *ca.* 20 K, and this is not well reproduced by the model. Others have used a similar spin–spin model to that employed here, on related species.[53] Strictly, octahedral iron(II) centres have $^5T_{2g}$ ground states and the Heisenberg model is not appropriate. However, under ligand-field distortions of the type anticipated in the present structure, it is reasonable to assume a $^5B_2$ ground state well separated from the ^5E, possibly with zero-field splitting (D) of the $^5B_2$ state. The simple model used here assumes $J >> D$. This seemed a reasonable approach since the complex was EPR silent when measured in transverse detection mode at both X-band at 4 K and Q-band at 100 K in the solid and frozen solution [acetonitrile–toluene (1:1)] states. However, use of high frequency ($\nu \geqslant 95$ GHz) and/or parallel detection mode for even-spin-state signals, of the type pioneered by Hendrich and co-workers,[54] would be required to confirm this. The inflection in the χ_m plot at *ca.* 20 K probably relates to zero-field splitting or to the presence of some μ-oxo-diiron(III) impurity. There was no evidence for the μ-oxo species in the Mössbauer spectrum. Proof of zero-field splitting would require variable-field measurements in the temperature range 50–2 K, in the manner used recently for $S = 2$ dimers[55] and monomers,[56] and analysis by a spin Hamiltonian containing J and D terms.[54–56] This was not done in the present study since the primary aim was to deduce the J value which is clearly defined by the position of χ_{max} and by the use of the simple $-2JS_1 \cdot S_2$ model.

The modest antiferromagnetic coupling observed for $[Fe_2(OH)(O_2CMe)_2(Me_2[9]aneN_2S)_2]ClO_4$ is consistent with the exchange coupling observed in OR-bridged binuclear iron(II) complexes (OR = hydroxide, alkoxide or phenoxide),[51,57,58] for example $[Fe_2(OH)(O_2CMe)_2(Me_3[9]aneN_3)_2]ClO_4$ ($J = -13$ cm^{-1})[13] and with deoxy proteins, *e.g.* deoxyhaemerythrin (-13 cm^{-1}).[1] Contrastingly, complexes that contain a μ-aqua bridge, such as $[Fe_2(tmen)_2(H_2O)(O_2Ph)_4]$ and $[Fe_2(tmen)_2(H_2O)(O_2Ph)_4]$ (tmen = $Me_2NCH_2CH_2NMe_2$), exhibit small ferromagnetic or weak exchange.[59] The weak exchange in the protonated binuclear iron(II) complex is in line with the concept that the μ-hydroxo moiety is a weak mediator of the π-superexchange pathway. This is clearly illustrated in the attenuation of the exchange coupling between binuclear μ-oxo-diiron(III) complexes upon protonation of the bridging oxo group.[60–62]

The mechanism of the exchange interaction in binuclear iron(II) complexes has not been investigated as extensively as for the binuclear μ-oxo-diiron(III) complexes. Recently, Hendrich and co-workers[54] prepared a series of binuclear complexes bridged by a μ-phenoxo and bis(μ-carboxylato) or bis(μ-phosphato) core. The μ-phosphato-bridged complex $[Fe_2L\{O_2P(OPh)_2\}_2]BF_4$ (L = 2,6-bis{[bis(2-pyridylmethylamino]-methyl}-4-methylphenol) had a larger Fe–O–Fe angle [122.7(2)°] and displayed antiferromagnetic coupling, compared to the μ-propionato analogue [108.93(6)°] which exhibited ferromagnetic coupling.[54] The change from ferro- to antiferromagnetic behaviour was attributed to the larger M–O–M angle, the modulation of the coupling in the diiron(II) system being apparently similar to that for dicopper(II) complexes.[54,63] Whilst it is clear that the Fe–O–Fe angle is important for the diiron(II) complexes, the limited number of examples of these leaves the exact influence of the Fe^{II}–μ-O bond distance on the exchange interaction to be established.[54] Zero-field splitting effects, of the type alluded to above, further complicate the picture.

Electrochemistry

The electrochemical properties of $[Fe_2O(O_2CMe)_2([9]aneN_2S)_2][PF_6]_2$ and $[Fe_2O(O_2CMe)_2(Me_2[9]aneN_2S)_2][PF_6]_2$ were investigated using cyclic voltammetry. The former complex exhibited a reduction wave at -0.760 V (*vs.* ferrocene–ferrocenium, 0.050 V s^{-1}) with a shoulder to positive potential at a scan rate of 0.100 V s^{-1}. As the scan rate was reduced the magnitude of the peak at -0.760 V decreased and the shoulder became the major peak at a scan rate of 0.010 V s^{-1}, with a peak potential at -0.610 V. Both processes were irreversible, although a small anodic inflection at -0.520 V was observed at high scan rates (<0.500 V s^{-1}). As the scan range is increased to -1.5 V another peak is observed at -1.050 V. The redox chemistry of $[Fe_2O(O_2CMe)_2(Me_2[9]aneN_2S)_2][PF_6]_2$ is less complicated and displays a quasi-reversible electron-transfer process in acetonitrile at $E_{\frac{1}{2}}$ of -0.556 V with ΔE of 0.140 V and I_c/I_a 1.26 (0.020 V s^{-1}).

The electrochemical behaviour of $[Fe_2O(O_2CMe)_2([9]aneN_2S)_2][PF_6]_2$ suggested that there were multiple species present in the electron transfer, with the second species ($E_c = -0.610$ V) being observed when the scan rate was decreased. The behaviour is indicative of a mechanism where the heterogenous electron transfer forming the reduced species is followed by a chemical reaction, with the reduced species reacting to form an electroinactive species, leaving only a small amount of the reduced species available for oxidation on the reverse sweep.[64] The peak observed at -1.050 V is assigned to the second reduction of the binuclear iron(III) dimer, *i.e.* the $Fe^{III/II} \rightleftharpoons Fe^{II/II}$ redox couple. Additionally, a small peak observed at approximately 0.4 V corresponds to the redox couple of $[Fe([9]aneN_2S)_2]^{2+/3+}$ arising from reductive decom-

position of $[Fe_2O(O_2CMe)_2([9]aneN_2S)_2][PF_6]_2$. Continuous scans failed to produce an increase of the peak current indicating this was not the major product after reduction, in contrast to the situation for $[Fe_2O(O_2CMe)_2\{HB(pz)_3\}_2]$ which displayed an irreversible process in acetonitrile at −1.182 V and a couple assigned to the mononuclear complex $[Fe\{HB(pz)_3\}_2]^{+/2+}$ ($E_{\frac{1}{2}}$ 0.192 V) as a result of decomposition of the dimer.[65]

The quasi-reversible electron-transfer process displayed by $[Fe_2O(O_2CMe)_2(Me_2[9]aneN_2S)_2][PF_6]_2$ at −0.556 V is assigned to the $Fe^{III}Fe^{III}$–$Fe^{II}Fe^{III}$ couple, the reversibility being attributed to the fact that the methylated derivative is less likely to form mononuclear complexes upon reduction due to the steric constraints of the methyl substituents. Similar electrochemical behaviour was reported for $[Fe_2O(O_2CMe)_2(Me_3[9]aneN_3)_2]^{2+}$.[14] Very recently,[66] the mixed-valence complex $[Fe^{III}Fe^{II}(\mu\text{-}OH)(\mu\text{-}O_2CCMe_3)_2(Me_3[9]aneN_3)_2]^{2+}$ has been structurally characterised and found to have properties similar to semi-methaemerythrin. It forms the μ-oxo-diiron(III) analogue in air, and thus protonation equilibria probably occur simultaneously with electron transfer.

Incorporation of the thioether in these tridentate cyclononane macrocycles shifts the redox couple to positive potential, stabilising the lower oxidation state, Fe^{II}.

Acknowledgements

We thank Mr. Yasser Korbatieh and Professor John D. Cashion for the measurement and analysis of the Mössbauer spectrum.

References

1 K. K. Andersson and A. Gräslund, *Adv. Inorg. Chem.*, 1995, **43**, 359.
2 R. Hotzelmann, K. Wieghardt, U. Flörke, H.-J. Haupt, D. C. Weatherburn, J. Bonvoisin, G. Blondin and J.-J. Girerd, *J. Am. Chem. Soc.*, 1992, **114**, 1681.
3 R. Hotzelmann, K. Wieghardt, J. Ensling, H. Romstedt, P. Gütlich, E. Bill, U. Flörke and H.-J. Haupt, *J. Am. Chem. Soc.*, 1992, **114**, 9470.
4 B. Mauerer, J. Crane, J. Schuler, K. Wieghardt and B. Nuber, *Angew. Chem., Int. Ed. Engl.*, 1993, **32**, 289.
5 P. Chaudhuri, M. Winter, P. Fleischhauer, W. Haase, U. Flörke and H.-J. Haupt, *Inorg. Chim. Acta*, 1993, **212**, 241.
6 S. Drüeke, P. Chaudhuri, K. Pohl, K. Wieghardt, X.-Q. Ding, E. Bill, A. Sawaryn, A. X. Trautwein, H. Winkler and S. J. Gurman, *J. Chem. Soc., Chem. Commun.*, 1989, 59.
7 P. Chaudhuri, M. Winter, K. Wieghardt, S. Gehring, W. Haase, B. Nuber and J. Weiss, *Inorg. Chem.*, 1988, **27**, 1564.
8 A. Spool, I. D. Williams and S. J. Lippard, *Inorg. Chem.*, 1985, **24**, 2156.
9 K. Wieghardt, I. Tolksdorf and W. Herrmann, *Inorg. Chem.*, 1985, **24**, 1230.
10 J. L. Sessler, J. W. Sibert, V. Lynch, J. T. Markert and C. L. Wooten, *Inorg. Chem.*, 1993, **32**, 621.
11 J. L. Sessler, J. W. Sibert and V. Lynch, *Inorg. Chem.*, 1990, **29**, 4143.
12 P. Poganiuch, S. Liu, G. C. Papaefthymiou and S. J. Lippard, *J. Am. Chem. Soc.*, 1991, **113**, 4645.
13 K. Wieghardt, K. Pohl and W. Gebert, *Agnew. Chem., Int. Ed. Engl.*, 1983, **22**, 727.
14 J. R. Hartman, R. L. Rardin, P. Chaudhuri, K. Pohl, K. Wieghardt, B. Nuber, J. Weiss, G. C. Papaefthymiou, R. B. Frankel and S. L. Lippard, *J. Am. Chem. Soc.*, 1987, **109**, 7387.
15 K. Wieghardt, K. Pohl and D. Ventur, *Angew. Chem., Int. Ed. Engl.*, 1985, **24**, 392.
16 G. C. Silver and W. C. Trogler, *J. Am. Chem. Soc.*, 1995, **117**, 3983.
17 T. Jüstel, T. Weyhermüller, K. Wieghardt, E. Bill, M. Lengen, A. X. Trautwein and P. Hildebrandt, *Angew. Chem., Int. Ed. Engl.*, 1995, **34**, 669.
18 J. I. Bruce, T. M. Donlevy, L. R. Gahan, C. H. L. Kennard and K. A. Byriel, *Polyhedron*, 1995, **15**, 49.
19 T. M. Donlevy, L. R. Gahan, T. W. Hambley, G. R. Hanson, K. L. McMahon and R. Stranger, *Inorg. Chem.*, 1994, **33**, 5131.
20 T. M. Donlevy, L. R. Gahan and T. W. Hambley, *Inorg. Chem.*, 1994, **33**, 2668.
21 J. I. Bruce, L. R. Gahan, T. W. Hambley and R. Stranger, *Inorg. Chem.*, 1993, **32**, 5997.
22 T. M. Donlevy, L. R. Gahan, R. Stranger, S. E. Kennedy, K. A. Byriel and C. H. L. Kennard, *Inorg. Chem.*, 1993, **32**, 6023.
23 T. M. Donlevy, L. R. Gahan, T. W. Hambley, K. L. McMahon and R. Stranger, *Aust. J. Chem.*, 1993, **46**, 1799.
24 J. I. Bruce, L. R. Gahan, T. W. Hambley and R. Stranger, *J. Chem. Soc., Chem. Commun.*, 1993, 702.
25 L. R. Gahan, G. A. Lawrance and A. M. Sargeson, *Aust. J. Chem.*, 1982, **35**, 1119.
26 E. K. Barefield and F. W. Wagner, *Inorg. Chem.*, 1973, **12**, 2435.
27 SDP Structure Determination Package, Enraf-Nonius, Delft, 1985.
28 G. M. Sheldrick, SHELXS 86, in *Crystallographic Computing 3*, eds. G. M. Sheldrick, C. Krüger and R. Goddard, Oxford University Press, Oxford, 1985, pp. 175–189.
29 G. M. Sheldrick, SHELX 76, Program for Crystal Structure Determination, University of Cambridge, 1976.
30 D. T. Cromer and J. T. Waber, *International Tables for X-Ray Crystallography*, Kynoch Press, Birmingham, 1974, vol. 4.
31 C. K. Johnson, *ORTEP, A Thermal Ellipsoid Plotting Program*, Oak Ridge National Laboratory, Oak Ridge, TN, 1965.
32 W. H. Armstrong and S. J. Lippard, *J. Am. Chem. Soc.*, 1983, **105**, 4837.
33 P. Chakraborty, S. K. Chandra and A. Chakravorty, *Inorg. Chem.*, 1994, **33**, 6429.
34 A. J. Blake, A. J. Holder, T. I. Hyde and M. Schröder, *J. Chem. Soc., Chem. Commun.*, 1989, 1433.
35 T. Mashiko, C. A. Reed, K. J. Haller, M. E. Kastner and W. R. Scheidt, *J. Am. Chem. Soc.*, 1981, **103**, 5758.
36 S.-H. Cho, D. Whang, K.-N. Han and K. Kim, *Inorg. Chem.*, 1992, **31**, 519.
37 J. K. Beattie and C. J. Moore, *Inorg. Chem.*, 1982, **21**, 1292.
38 L. Que, jun. and A. E. True, *Prog. Inorg. Chem.*, 1990, **38**, 97.
39 D. M. Kurtz, jun., *Chem. Rev.*, 1990, **90**, 585.
40 A. L. Feig and S. J. Lippard, *Chem. Rev.*, 1994, **94**, 759.
41 C. Cheng and W. M. Reiff, *Inorg. Chem.*, 1977, **16**, 2097.
42 C. J. O'Connor, *Prog. Inorg. Chem.*, 1982, **29**, 203.
43 J. B. Vincent, J. C. Huffman, G. Christou, Q. Li, M. A. Nanny, D. N. Hendrickson, R. H. Fong and R. H. Fish, *J. Am. Chem. Soc.*, 1988, **110**, 6898.
44 B. J. Kennedy, K. S. Murray, P. R. Zwack, H. Homborg and K. Kalz, *Inorg. Chem.*, 1985, **24**, 3302.
45 C. Ercolani, M. Gardini, K. S. Murray, G. Pennesi and G. Rossi, *Inorg. Chem.*, 1986, **25**, 3972.
46 R. N. Mukherjee, T. P. D. Stack and R. H. Holm, *J. Am. Chem. Soc.*, 1988, **110**, 1850.
47 S. M. Gorun and S. J. Lippard, *Inorg. Chem.*, 1991, **30**, 1625.
48 S. Drüeke, K. Wieghardt, B. Nuber and J. Weiss, *Inorg. Chem.*, 1989, **28**, 1414.
49 K. Tatsumi and R. Hoffman, *J. Am Chem. Soc.*, 1981, **103**, 3328.
50 P. J. Hay, J. C. Thibeault and R. Hoffman, *J. Am. Chem. Soc.*, 1975, **97**, 4884.
51 B. S. Synder, G. S. Patterson, A. J. Abrahamson and R. H. Holm, *J. Am. Chem. Soc.*, 1989, **111**, 5214.
52 P. Gomez-Romero, E. H. Witten, W. M. Reiff and G. B. Jameson, *Inorg. Chem.*, 1990, **29**, 5211.
53 Y. Hayashi, T. Kayatani, H. Sugimoto, M. Suzuki, K. Inomata, A. Uehara, Y. Mizutani, T. Kitagawa and Y. Maeda, *J. Am. Chem. Soc.*, 1995, **117**, 11 220.
54 H. G. Jang, M. P. Hendrich and L. Que, jun., *Inorg. Chem.*, 1993, **32**, 911.
55 Y. Dong, S. Ménage, B. A. Brennan, T. E. Elgren, H. G. Jang, L. L. Pearce and L. Que, jun., *J. Am. Chem. Soc.*, 1993, **115**, 1851.
56 B. J. Kennedy and K. S. Murray, *Inorg. Chem.*, 1985, **24**, 1552.
57 A. Stassinopoulos, G. Schulte, G. C. Papaefthymiou and J. P. Caradonna, *J. Am. Chem. Soc.*, 1991, **113**, 8686.
58 S. Menage, B. A. Brennan, C. Juarez-Garcia, E. Münck and L. Que, jun., *J. Am. Chem. Soc.*, 1990, **112**, 6423.
59 K. S. Hagen and R. Lachicotte, *J. Am Chem. Soc.*, 1992, **114**, 8741.
60 W. H. Armstrong and S. J. Lippard, *J. Am. Chem. Soc.*, 1984, **106**, 4632.
61 M. Rapta, P. Kamaras, G. A. Brewer and G. B. Jameson, *J. Am. Chem. Soc.*, 1995, **117**, 12 865.
62 R. Hazell, K. B. Jensen, C. J. McKenzie and H. Toftlund, *J. Chem. Soc., Dalton Trans.*, 1995, 707.
63 W. E. Hatfield, in *Magneto-structural Correlations in Exchange Coupled Systems*, eds. R. D. Willet, D. Gatteschi and O. Kahn, Reidel, New York, 1983.
64 A. J. Bard and L. R. Faulkner, *Electrochemical Methods*, Wiley, New York, 1980.
65 W. H. Armstrong, A. Spool, G. C. Papaefthymiou, R. B. Frankel and S. J. Lippard, *J. Am. Chem. Soc.*, 1984, **106**, 3653.
66 U. Bossek, H. Hummel, T. Weyhermüller, E. Bill and K. Wieghardt, *Angew. Chem., Int. Ed. Engl.*, 1995, **34**, 2642.

Received 22*nd July* 1996; *Paper* 6/05058A